ADVANCES IN THERMAL HYDRAULICS OF OXYGEN PRODUCTION REACTORS IN THE COPPER-CHLORINE CYCLE FOR HYDROGEN PRODUCTION: A COMPREHENSIVE REVIEW

Mohammed Wassef Abdulrahman
Rochester Institute of Technology
Dubai / UAE

ABSTRACT: The thermochemical water splitting process using the copper-chlorine (Cu-Cl) cycle is an innovative method for generating hydrogen gas. This process involves a thermolysis reaction where molten salt, a solid reactant, and gaseous oxygen interact to produce oxygen gas. The primary aim of this work is to contribute to the development and enhancement of the thermochemical Cu-Cl cycle for hydrogen production. To achieve this goal, a comprehensive review of the multiphase oxygen generation reactor, which is a crucial component of the Cu-Cl cycle, is conducted. The review covers various aspects of the oxygen reactor, including; type and description of the Oxygen reactor, material features, variables affecting reactor's size, and scale-up evaluations. This work aims to provide a thorough understanding of the oxygen reactor in the Cu-Cl cycle, highlighting its significance in the thermochemical production of hydrogen and the key considerations for its optimization and scale-up.

INTRODUCTION

Hydrogen is increasingly recognized as a pivotal solution to the environmental challenges posed by greenhouse gas emissions, which are largely attributed to the global dependence on fossil fuels. It is widely regarded as a significant contributor to the future sustainable energy supply, as its utilization can substantially reduce atmospheric pollution and mitigate climate change by lowering greenhouse gas emissions (Forsberg, 2007). Given its versatile applications across various industries, the demand for hydrogen is projected to rise considerably in the forthcoming decade.

The majority of hydrogen production on a global scale currently relies on methods such as steam-methane reforming or partial oxidation of heavy hydrocarbons. While these processes are efficient, they generate substantial quantities of carbon

dioxide, contributing to greenhouse gas emissions. These conventional methods are facing increasing challenges due to escalating greenhouse gas emissions, reducing natural gas resources, and rising costs associated with carbon capture and storage.

In light of the exponential growth in demand for hydrogen, the primary challenge for the hydrogen economy is the sustainable generation of hydrogen on a large scale, without dependence on fossil fuels, and at costs lower than those of existing technologies. In this context, nuclear energy emerges as a potential source for large-scale, sustainable hydrogen production.

Thermochemical cycles represent a promising alternative that can be integrated with nuclear reactors to thermally decompose water into oxygen and hydrogen through a series of intermediate processes. These cycles facilitate the transfer of heat between different reactors, some of which are endothermic and others exothermic, via heat exchangers that either provide or recover heat from specific processes. The copper-chlorine (Cu-Cl) cycle, identified by Argonne National Laboratories (ANL) as one of the most promising low-temperature cycles, stands out in this regard (Lewis et. al 2003; Serban et. al., 2004). One of the most notable advantages of the Cu-Cl cycle is its lower temperature requirement compared to many other cycles, which enhances its efficiency and accessibility. Furthermore, the cycle can be conducted in a manner that necessitates minimal high-quality energy and solid exchanges, making it more environmentally and economically viable.

The integration of this cycle with nuclear energy offers a sustainable pathway for hydrogen generation, addressing the pressing need for clean energy solutions. As the world moves towards a more sustainable energy future, the development and optimization of thermochemical cycles like the Cu-Cl cycle, in conjunction with advancements in nuclear technology, hold great promise for meeting the growing demand for hydrogen while mitigating the environmental impact of energy production. This cycle comprises three reactions: two thermal and one electrochemical. The Cu-Cl cycle comprises three reactions, two thermal and one electrochemical:

$CuCl\ (a) + 2HCl\ (g) \rightarrow CuCl_2\ (a) + H_2\ (g)$	100°C	step (1)	(1)
$2CuCl_2\ (s) + H_2O\ (g) \leftrightarrow Cu_2OCl_2\ (s) + 2HCl\ (g)$	375°C	step (2)	(2)
$Cu_2OCl_2\ (s) \rightarrow 2CuCl\ (l) + ½\ O_2\ (g)$	530°C	step (3)	(3)
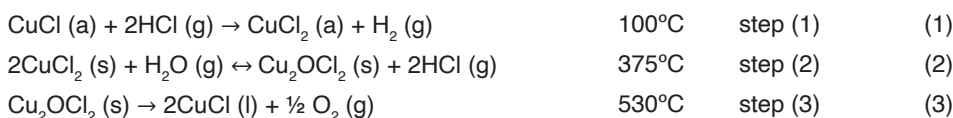
where *a*, *s*, *l* and *g* denote to aqueous, solid, liquid and gas respectively.

In the oxygen generation stage (step 3), an intermediate chemical known as solid copper oxychloride (Cu_2OCl_2) undergoes decomposition, resulting in the formation of oxygen gas and molten cuprous chloride (CuCl). This stage is crucial for the overall efficiency of the Cu-Cl cycle. The oxygen generation reactor receives an input of anhydrous solid Cu_2OCl_2 from the preceding step in the cycle, which is the hydrolysis of CuCl2. This hydrolysis process operates at temperatures ranging from 350 to 450°C. Once inside the oxygen reactor, the solid Cu_2OCl_2 is subjected to higher temperatures, typically between 450 and 530°C, which triggers its decomposition into oxygen gas and molten CuCl.

However, the process is not without its challenges. The gaseous output from the oxygen reactor may include not only the desired oxygen gas but also potential contaminants from side reactions. These could include vaporized CuCl, chlorine gas, and trace amounts of hydrochloric acid (HCl) gas and water vapor (H_2O). These by-products need to be carefully managed to ensure the purity of the produced oxygen and the overall efficiency of the cycle.

Moreover, the substances exiting the reactor are primarily molten CuCl, but there might also be solid $CuCl_2$ present. This can occur due to the incomplete breakdown of $CuCl_2$ at temperatures below 750°C (Micco et. al., 2007). Additionally, reactant particles may be entrained in the flow of molten CuCl, further complicating the process.

Overall, the oxygen generation stage of the Cu-Cl cycle is a complex process that requires careful control and management to ensure its efficiency and effectiveness in contributing to the sustainable production of hydrogen.

OXYGEN REACTOR TYPE

Three phases comprise the oxygen reactor: the solid phase (copper oxychloride particles), the liquid phase (molten salt), and the leaving gaseous phase (oxygen). In chemical, petroleum, and biological processes, multiphase reactions such as gas/liquid/solid are often employed. The industry offers various different kinds of multiphase reactors, which may be grouped into two broad categories: fixed bed reactors and slurry phase reactors. Fixed bed or packed bed reactors have a stationary solid phase. Because the oxygen reactor's solid phase is continuous, it cannot be termed a fixed bed reactor (Abdulrahman, 2016a). Stirred tank reactors (STR) and slurry bubble column reactors are the most common continuous slurry phase reactors (SBCRs). The continuous stirred tank reactor (CSTR), which is often used for liquid-phase or multiphase processes with moderate reaction rates, is a mechanically agitated reactor in which small particles are suspended in the liquid phase by agitation. Continuous reaction streams are supplied into the vessel, while product streams are removed. In general, a continuous flow stirred tank reactor (CFSTR) implies that the fluid is properly mixed, ensuring that the reaction mixture's parameters (e.g., concentration, density, and temperature) remain uniform throughout the system. As a result, the conditions throughout the reactor are same, and the temperature at the reactor output is identical. The solid phase in the SBCR is composed of small particles suspended in the liquid phase as a result of gaseous bubbles supplied from the bottom, often through a sparger (Abdulrahman, 2016a; Li et. al., 2016).

Oxygen reactors may be classified as CFSTRs or SBCRs. The decision between these two kinds of reactors is determined by the heat transfer rate efficiency, the agitation efficiency, the ability to scale up, and other design requirements. The oxygen reactor's thermal design demands adequate agitation inside the reactor and a sufficiently high rate of heat transfer to the solid particles. Agitation may be accomplished mechanically, as

in the CFSTR, or by gaseous bubbles, as in the SBCR. Although the rate of agitation is faster with a mechanical agitator than with bubbles, an agitator is undesirable in a highly corrosive medium such as an oxygen reactor due to the numerous internals required, such as the propeller, shaft, baffles, and other accessories that support the mixing system (Abdulrahman, 2016a).

Heating may be accomplished in two ways: indirectly or directly. The two most often used indirect procedures are to surround the vessel with a jacket or to use an inside coil. Direct heating may be accomplished by the use of gaseous bubbles and is more efficient than indirect heating, but is more complicated to scale up. The oxygen gas that exits the oxygen reactor at around 530°C may be heated to a higher temperature (such as 600°C) and then re-injected into the oxygen reactor from the bottom through a sparger. Direct contact heat transfer between the hot oxygen gas and the slurry within the oxygen reactor is possible in this instance (Abdulrahman, 2016a).

According to the comparison above, SBCR is more efficient in heat transmission than CFSTR but more difficult to scale up. However, with SBCR, thermal energy may be delivered to the reactor directly through gas bubbles, which can also be utilized to agitate the reactor's contents.

OXYGEN REACTOR SYSTEM DESCRIPTION

As with many chemical reactors, the oxygen reactor needs careful regulation of heat transfer to operate at peak efficiency. Cu_2OCl_2 decomposition into oxygen and molten CuCl is an endothermic process in the oxygen reactor, requiring a reaction heat of 129.2 kJ/mol and a temperature of 530°C, the highest temperature in the Cu-Cl cycle. As a result, heat must be provided to increase and maintain the temperature of the reactor's bulk (Ryskamp, 2004). The total amount of heat needed is the sum of reaction heat and the heat necessary to elevate the reactant temperature from 375°C (the temperature of solid particles formed during the hydrolysis process) to 530°C. The heat transfer coefficient, the difference between the bulk and surrounding temperatures of the heat transfer fluid (i.e., the driving force), and the size of the contact region where the heat transfer occurs all affect the heat transfer. Additionally, the heat transfer coefficient is dependent on the oxygen generation process's operating conditions, the physical qualities of the inventory materials, and the geometry of the equipment. Typically, this coefficient is established by the use of empirical correlations.

The oxygen reaction is a high temperature reaction that requires a source of high temperature heat. This heat may be generated by generation IV nuclear reactor designs such as the sodium-cooled reactor, the Canada Deuterium Uranium (CANDU) supercritical water reactor (CANDU-SCWR), Canada's Generation IV reactor, and the high temperature gas reactor (HTGR). While the first two reactors operate at lower temperatures (510°C – 625°C), they are ideally suited for matching a low temperature Cu-Cl thermochemical

cycle. However, coupling low temperature cycles to the HTGR (1000°C) may enable more cogeneration, resulting in much better hydrogen production efficiency. Solar energy is another non-polluting source of high-temperature heat.

In an indirect cycle system, an intermediate heat exchanger (IHX) is utilized to transmit heat from the main fluid in the nuclear reactor core to the secondary fluid, which then delivers the heat to the hydrogen plant's oxygen reactor. Helium, a nitrogen/helium combination, or a molten salt may be used as the secondary fluid. IHX is designed to collect heat from the main fluid at the maximum temperature achievable (the reactor output temperature) for use in the hydrogen generation process. Harvego (2006) studied several setups for an intermediate heat exchanger between a hydrogen generation cycle and an NGNP. The flow rates, temperature distribution across the loops, and other IHX needs were also suggested based on the design, and the reactor output temperature was set at 900°C in earlier research by Natesan et al. (2006).

MATERIAL PROPERTIES OF OXYGEN REACTOR

Ikeda and Kaye (2008), as well as Trevani et al. (2011), have investigated the thermochemical characteristics of copper oxychloride. Because copper oxychloride is not commercially accessible, these two investigations discovered strategies for its manufacture. Ikeda and Kaye (2008) used stoichiometric quantities of CuO and $CuCl_2$ in their approach. To prevent the presence of moisture, the procedure was carried out in a glove box filled with argon. Trevani et al. (2011) used a more straightforward method. Cu_2OCl_2 was created in their approach using a typical horizontal tube furnace equipped with a quartz tube and stainless-steel gas injection connectors. CuCl or $CuCl_2$ was placed into an alumina crucible and subjected for 48 hours to a flow of high-quality dry air at 370°C. The X-Ray Diffraction (XRD) analysis indicated that this approach produced very pure Cu_2OCl_2 samples. The approach is more scalable, and it is capable of producing the quantities necessary for large-scale oxygen generation tests. Cu_2OCl_2 is a solid that decomposes in the presence of water, hence it is essential to preserve it under nitrogen or dry air.

Parry (2008) reported calorimetric measurements of copper oxychloride's heat capacity in the range of 20-410°C. The Debbiee-Einstein technique was used to extrapolate thermodynamic data to 550°C. Uncertainty developed in the low-temperature range due to the quick change in heat capacity in this area. The slope of the calorimetric specific heat curve drops to less than 5 J/mol.K every 100°C above 400°C. Differences in observed data were attributed to undetected heat leakage. The standard deviation of results acquired using this approach was calculated to be 1.1%.

Abdulrahman (2016a, 2019a, 2020a) has derived a linear function of CuCl surface tension with temperature as follows:

$$\sigma_{CuCl} = 0.115 - 5.312 \times 10^{-5} \, T \qquad\qquad (4)$$

The derivation was based on the approximate linear reduction of the surface tension with temperature and the equality of the surface tension to zero at the critical temperature of the liquid. The critical temperature that is used in deriving Eq. (4) is equal to 2435 K. The surface tension of molten CuCl in contact with air is equal to 0.092 N/m at the melting temperature of CuCl (430°C) (Janz and Tomkins, 1983).

There are various obstacles and challenges in utilizing the real materials from the thermolysis reactor products in the experimental research for the scale up analysis (i.e. molten salt CuCl and oxygen gas). Abdulrahman (2016a, 2019a, 2020a) developed alternative materials by simulating the hydrodynamic and heat transport characteristics of actual materials utilizing dimensional analyses of the Buckingham pi theorem. These alternate materials have been identified as liquid water at a temperature of 22°C and helium gas at a temperature of 90°C. The physical properties for He gas and liquid water are shown in Table 1 (Abdulrahman, 2016a). Alternative materials offer a safe environment for experimental runs and operate at a lower temperature. Additionally, these materials are readily available and inexpensive. Abdulrahman's material simulation is a unique tool for assessing hydrodynamic and heat transport behaviours in a simulated environment prior to adaptation to the Cu-Cl cycle thermolysis reactor.

Physical Property	Unit	Gas Phase (He)	Liquid Phase (H_2O)
Temperature (T)	°C	90	22
Temperature (T)	K	363	295
Density (ρ)	kg/m³	0.1344	998.2
Specific Heat (C_p)	J/kg K	5193	4182
Thermal Conductivity (k)	W/m K	0.1687	0.6
Dynamic Viscosity (μ)	kg/m s	2.267E-5	0.000975
Molecular Weight	kg/ kmol	4.0026	18.0152
Standard State Enthalpy	J/ kg mol	-	-2.858e+8
Surface Tension (σ)	N/m	-	0.0724

Table 1: Material properties for the Helium gas and liquid Water (Abdulrahman, 2016a).

OXYGEN PRODUCTION CHEMICAL REACTION

Experiments were carried out to determine the volatility of CuCl and the products of Cu_2OCl_2 decomposition. Copper oxychloride retained its chemical characteristics at temperatures up to 370°C. Cl_2 was released between 375°C and 470°C during the production of CuCl. Cl_2 then reacted with CuO to form oxygen and CuCl, as well as trace quantities of unreacted $CuCl_2$. Between 475°C and 550°C, XRD analysis demonstrated an increase in the quantity of $CuCl_2$ in the products, whereas the amount of CuO decreased. The decomposition reaction (called path I) has the following form:

$$Cu_2OCl_2 \rightarrow CuCl + CuO + \tfrac{1}{2} Cl_2 \qquad (5)$$
$$CuO + Cl_2 \rightarrow CuCl_2 + \tfrac{1}{2} O_2 \qquad (6)$$
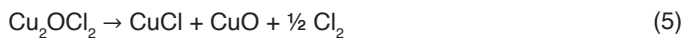
Parallel to the competitive reaction, experimental data suggested that the secondary reaction was responsible for the partial drop in CuO caused by the Cl_2 generated in the former reaction. This collection was named "reaction "path I." Another way to generate oxygen is by the decomposition of a combination of CuO and $CuCl_2$, as Serban et al. investigated (Serban et. al., 2004). The studies were conducted in a vertical reactor at 500°C using an equimolar combination of CuO and $CuCl_2$. The XRD measurement of the solid products revealed a pure CuCl solid phase. The investigation used a mechanistic approach and determined that oxygen evolution is constrained by $CuCl_2$ decomposition. As specified in the following equations "path II," the reaction proceeded in two steps.

$$CuCl_2 \ (s) \rightarrow CuCl \ (s) + \tfrac{1}{2} Cl_2 \ (g) \qquad (7)$$
$$CuO \ (s) + \tfrac{1}{2} Cl2 \ (g) \rightarrow CuCl \ (s) + \tfrac{1}{2} O_2 \ (g) \qquad (8)$$
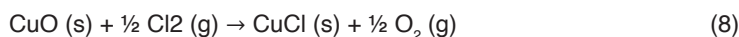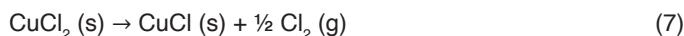
The competing reaction in Eq. (7) is cupric chloride's heterogeneous and endothermic thermolysis. Even while only 60% decomposition of $CuCl_2$ occurs at 530°C, the addition of CuO seems to enhance decomposition. Additionally, it was found that the Cl_2 produced is completely consumed in the reaction with CuO, as indicated by Eq. (8), since no free Cl_2 was found in the gaseous products. The Gibbs free energy of the reaction suggests that it enters equilibrium around 500°C and then proceeds spontaneously, with increasing amounts of chlorine available to react with CuO as the temperature rises. However, experimental data suggested that $CuCl_2$ does not completely decompose until it reaches 600°C.

Lewis et al. (2005) utilized 40 mg of laboratory-produced Cu_2OCl_2 heated to 530°C for the oxygen generation process in their experiment. Based on the quantity of copper oxychloride used in the experiment, it was found that the observed mass of oxygen was more than the theoretical limit. The presence of chlorine peaks was found to be below background values. Lewis et al. (2003, 2019) utilized a stoichiometric combination of CuO and $CuCl_2$ heated to 500°C to achieve an oxygen output of 85%. The X-ray diffraction (XRD) analysis of products revealed the presence of CuCl and negligible levels of $CuCl_2$. At 500°C, 0.02 mol of an equimolar combination of CuO and dehydrated $CuCl_2$ was decomposed in a separate experiment. The oxygen production was more than what thermodynamic equilibrium studies expected. The amount of chlorine released was not determined. Continuous oxygen removal was used in the experiments. The XRD investigation of the solid products revealed the presence of CuCl and $CuCl_2$. The findings indicate that the oxygen released during copper oxychloride decomposition is more than the predicted yield from a combination of $CuCl_2$ and CuO. The reason chlorine was not found is unclear, however it might have been due to the presence of chlorine gas or a low yield of chlorine below the chlorine analyser's detection threshold.

Marin (2012) established a novel experimental and theoretical basis for scaling up a CuO*CuCl$_2$ decomposition reactor while considering the effect on the yield of the thermochemical copper-chlorine cycle for hydrogen production. He utilized a Stefan boundary condition in conjunction with a new particle model to monitor the location of the moving solid-liquid interface as the solid particle decomposes due to surface heat transfer. Thermo gravimetric Analysis (TGA) microbalance and laboratory scale batch reactor studies were used to investigate the conversion of CuO*CuCl$_2$ and estimate the rate of endothermic reaction. At high temperatures and low Reynolds numbers, a second particle model finds characteristics that affect the transient chemical decomposition of solid particles embedded in a bulk fluid composed of molten and gaseous phases. For a particle suddenly submerged in a viscous continuum, the mass, energy, momentum, and chemical reaction equations were solved. Numerical solutions were generated and evaluated using experimental data on the chemical decomposition of copper oxychloride (CuO*CuCl$_2$).

FACTORS AFFECTING OXYGEN REACTOR SIZE

There are many factors that affect oxygen reactor size. These factors include the residence time of the thermal decomposition for solid particles, terminal settling velocity of solid particles, production rate of hydrogen (mass balance), and reactor heating rate (heat balance) (Abdulrahman, 2016a, 2013a).

Terminal Settling Velocity of Particles

The amount of time it takes for solid particles to settle in a reactor with a limited volume is an essential metric to consider while designing the reactor (Felice and Kehlenbeck, 2000). The rate at which particles descend has a considerable impact on the height of the reactor. It is advised that the particle fall speed be kept as low as possible in order to provide adequate time for the decomposition process to be completed before reaching the bottom of the reactor. It is not necessary to have a high reactor in this situation.

Due to the fact that the density of the solid Cu$_2$OCl$_2$ particle is larger than that of molten CuCl, the falling velocity of a single particle under gravity will be greater than that of molten CuCl. The particle will continue to accelerate for a brief period and then descend at a constant velocity, where the effective weight of the particle and the drag force are identical. Thus, the most essential period is the period of constant-velocity descent (terminal settling velocity). The terminal velocity of solid particles is determined by a number of characteristics, including their size, shape (roundness), solid concentration and density, as well as the liquid's viscosity and density (Nguyen and Schulze, 2003).

Particle size: In industry, solid particles are often not uniform in size, but rather contain a variation of sizes. It is commonly established that bigger particles settle at a

faster rate than smaller ones. Baldi and Alaria (1978) indicated that when dealing with a distribution of particle sizes, it is appropriate to describe the particle diameter as the mass-mean diameter when computing the settling velocity.

Particle shape: In most theoretical computations, the form of solid particles is assumed to be spherical. The size of non-spherical particles may be described in terms of an equivalent volume of a sphere. A spherical particle's falling velocity is greater than that of a non-spherical particle with the same volume and density (Nguyen and Schulze, 2003).

Particle concentration: When a cloud of solid particles falls through a quiescent liquid, extra impeding actions have an impact on its falling velocity. These include the increased drag created by the close proximity of the particles inside the cloud and the liquid up flow induced by the falling particles. The impeding effects are highly dependent on the volumetric solid concentration in the cloud. The velocity of a hindered falling object is typically a fraction of the velocity of a free-falling object. For instance, with a solid concentration of 30% and a solid particle diameter range of 0.074-2 mm, the sand's impeded velocity is around 20%-40% of the single particle terminal velocity (Richardson and Zaki, 1954).

It is important to define in the design of the oxygen reactor's size if the settling velocity of the solid particles allows for sufficient residence time for complete decomposition of these particles before they settle to the reactor's bottom. It is widely established that the maximum settling velocity occurs when a single spherical particle falls infinitely deep into a fluid. Other factors such as particle shape, reactor wall, and impeding effects all contribute to the particles' settling velocity being reduced. The up-flow motion of the oxygen bubbles also reduces the fall of particles in the oxygen reactor.

Mass Production Rate of Hydrogen

In the design of any chemical reactor, it is necessary to study material balances (mass balances) which are based on the fundamental law of mass conservation. It is difficult to construct or run an oxygen reactor (or any other chemical plant) in a safe and cost-effective manner without proper material balances on hand. The general equation of the material balance is (Abdulrahman, 2016a, 2013a):

$$\frac{dm}{dt} = \dot{m}_i - \dot{m}_O + \dot{G} - \dot{C} \qquad (9)$$

where: $\frac{dm}{dt}$ is the rate of change of the material m, $\dot{m}_i$ and $\dot{m}_O$ are the inlet and outlet mass flow rates respectively, $\dot{G}$ and $\dot{C}$ are the rate of generation and consumption respectively. Abdulrahman et al. (2016a, 2013a) investigated the flow material balance for continuous processes running in the steady state. To produce hydrogen, they have investigated the flow rates and chemical compositions of all streams entering and exiting

each individual piece of equipment in the Cu-Cl cycle. It has been shown that the flow rate of each component of the Cu-Cl cycle (in the event of full conversion of the components) changes linearly with the rate of hydrogen production throughout the cycle.

Using varying residence times and hydrogen production rates, it was possible to compute the optimal size of an oxygen reactor. It was discovered that the size of the oxygen reactor changes linearly with the rate of hydrogen production and the residence time. According to the findings of Abdulrahman et al. (2016a, 2013a), the minimal size of the oxygen reactor can be determined based on the mass balance of the Cu-Cl cycle, and the size is strongly influenced by the residence time and hydrogen production rate of the reactor. Also, the size of the oxygen reactor was anticipated to be large because of the presence of copper (Cu), which has the maximum molecular weight of 63.54 g/mol in the Cu-Cl cycle, and hence the largest molecular weight in the Cu-Cl cycle.

METHOD OF HEATING OXYGEN REACTOR

A suitable method of heating the oxygen reactor is needed to provide enough heat that is necessary for solid decomposition. Heating the Cu_2OCl_2(s) particles only is undesirable, because of relatively slow rate of heat transfer. A more practical and efficient option is to heat the molten salt inside the oxygen reactor to in turn transfer the heat within the reactor from the liquid (molten CuCl) to the solid Cu_2OCl_2 (reactant) particles. The molten salt bath can be sustained by the reaction product itself. This approach is the most applicable and recommended one.

Due to buoyancy of the gas in the molten salt, the oxygen product will leave the reactant particles immediately. This fast separation aids to minimize heat transfer resistance to the reactant particles, which then helps make the overall reaction rate closer to the intrinsic reaction rate. The design of the reactor requires a high efficiency of heat exchange and separation of reactant (solid particles) from products, as well as one product (oxygen) from another (molten salt).

There are two main heating methods for reactor: electrical heating and fluid heating. The main disadvantage of electrical heating is the limited efficiency of electricity generation from nuclear heat (currently less than 35%). A more suitable method is to heat the molten salt by using a heating fluid (such as helium gas or molten salt) without using electricity.

Two main configurations of molten salt heating by a fluid can be used: direct and indirect heating. Direct heating places the heating fluid in direct contact with the heated medium. The advantage of heating directly is that, heating fluid is nearly 100% efficient with this method. This is because all heat that is generated is absorbed directly by the process. This helps to speed heat-up and eliminate thermal lag. There is no intermediate heat transfer medium that could result in heat losses. Direct heating can be applied by using a Slurry Bubble Column Reactor (SBCR), where the heating gas can be introduced to the reactor from the bottom through a sparger.

Indirect reactor heating uses a heat transfer medium to deliver the heat to the reactor vessel. Indirect methods can be external heating of the reactor using the reactor wall (or immersed tubes walls). There are various advantages of indirect heating. The biggest advantage is that the heating fluid can typically be serviced without draining the reactor. Second, indirect heating often allows watt density exposed to the process fluid, which is the number of watts concentrated per unit surface area of process side, to be lowered by spreading the heat over a larger surface. Finally, overheat conditions can be limited in many instances by simply limiting the temperature of the heat transfer medium, so that the process fluid is never exposed to temperatures higher than the heat transfer fluid temperature.

In spite of the above advantages, the disadvantages of indirect heating may be critical to the oxygen production process. The primary disadvantage is the thermal lag caused by using a heat transfer medium to carry the heat such as the reactor wall. The delay is caused by the fact that the heating fluid must first heat the heat transfer medium before the heat transfer medium can heat the process. If there is a large mass of heat transfer medium, larger heating capacities will be required to raise the temperatures.

Different types of indirect heat transfer surfaces can be used in an industrial oxygen reactor such as jackets, helical tubes immersed directly inside the reactor and vertical tube baffles (Oldshue, 1983). A reactor jacket is usually adequate to provide the required heat transfer surface for low and moderate heat duties (in terms of heat duty per unit of vessel volume). As heat duty increases, internal heat transfer surfaces (helical coils, baffle pipes, or plate coils) may be required.

Indirect Heat Transfer of the Oxygen Reactor

Thermal scaling up of the three-phase oxygen generation reactor in the Cu-Cl cycle was investigated using indirect heat transfer techniques (Abdulrahman, 2016a, 2016b, 2016c, 2019b, 2019c, 2013b, 2022a). The size of the oxygen reactor necessary to generate sufficient heat input was investigated in these researches for various hydrogen generation rates. The researches employed a continuous stirred tank reactor (CSTR) that was heated by a half pipe jacket (Abdulrahman, 2016a, 2016b) or an internal helical tube (Abdulrahman, 2016a, 2016c). The thermal resistance of each part of the reactor system was investigated in order to determine its influence on the reactor's heat balance. The system thermal resistance was found to be dominated by the reactor wall in jacketed reactors (Abdulrahman, 2016a, 2016b), and by the helical tube wall and service side in oxygen reactor systems with an internal helical tube (Abdulrahman, 2016a, 2016c).

The Cu-Cl cycle was assumed to be powered by a nuclear reactor in the above studies, and two different kinds of nuclear reactors were considered as a heat source for the oxygen reactor. The CANDU Super Critical Water Reactor (CANDU-SCWR) and the High Temperature Gas Reactor (HTGR) were two of these designs. It was established that a

larger heat transfer rate is required for CANDU-SCWR by three to four times that of HTGR, due to the HTGR's higher exit temperature, which results in greater temperature differential between the service and process sides than the SCWR.

From a thermal balancing standpoint, the impacts of reactor diameter and aspect ratio on the size of the oxygen reactor were calculated. It was determined that the size of the oxygen reactor reduces nonlinearly when the reactor diameter or aspect ratio increases, with the reactor diameter having a greater influence on the reactor size than the aspect ratio. The pace at which the oxygen reactor's size decreases was discovered to be slowed by increasing the reactor's diameter or aspect ratio.

On the service side, several kinds of working fluids were employed, including helium gas and CuCl molten salt, and their properties were compared. There is no discernible variation in the size of the jacketed oxygen reactor whether helium gas or CuCl molten salt is used (Abdulrahman, 2016a, 2016b). Due to the decrease in the number of oxygen reactors, it was established that utilizing CuCl molten salt in the service side is thermally superior to using helium gas in the oxygen reactor using an internal helical tube for heating (Abdulrahman, 2016a, 2016c). In general, both helium gas and CuCl molten salt have technical concerns, and both should be preserved and investigated until these technical difficulties are answered and an optimum decision can be chosen.

The findings of heat transfer studies conducted on the oxygen reactor with an internal helical tube were compared to the results of material balances and heat transfer analyses conducted on the oxygen reactor with a half pipe jacket. Due to the increased size needed for the heat balance, it was discovered that the size of the oxygen reactor is dictated by the heat balance rather than the material balance. Additionally, it was shown that delivering heat to the oxygen reactor through an internal helical tube is more efficient than utilizing a half pipe jacket.

Direct Contact Heat Transfer of the Oxygen Reactor

In examining the direct contact heat transfer within the oxygen reactor, comprehensive investigations were conducted utilizing both experimental and computational fluid dynamics (CFD) approaches (Abdulrahman, 2015, 2016a, 2016d, 2016e, 2016f, 2016g, 2018, 2020b,, 2020c, 2022b, 2022c, 2022d, 2023a, 2023b, 2023c). These studies aimed to understand and analyse the heat transfer mechanisms occurring within the reactor, where oxygen gas interacts directly with the other components, such as molten salt or solid particles.

The experimental studies involved setting up physical models of the oxygen reactor and conducting tests under controlled conditions to observe and measure the heat transfer rates, temperature profiles, and other relevant parameters. These experiments provided valuable data on how heat is transferred in the reactor, the influence of various operating conditions, and the effects of different reactor designs on the efficiency of heat transfer.

Concurrently, CFD studies were carried out to simulate the heat transfer processes within the oxygen reactor. Using Ansys Fluent software, detailed models of the reactor were created, incorporating the physical and chemical properties of the materials involved. These simulations allowed for a deeper analysis of the heat transfer phenomena, including the visualization of temperature distributions, gas holdup and flow patterns.

By combining the insights gained from both experimental and CFD studies, researchers aimed to optimize the design and operation of the oxygen reactor for improved heat transfer performance. This holistic approach ensures a more accurate and comprehensive understanding of the direct contact heat transfer mechanisms in the oxygen reactor, which is crucial for the development of more efficient and effective thermochemical processes for oxygen production.

Experimental Studies

Scaling up the thermolysis reactor requires a thorough understanding of hydrodynamics and heat transfer. However, using the actual products of the thermolysis reactor, such as molten salt CuCl and oxygen gas, presents several challenges in experimental studies on scaling up. These challenges include: 1) the high melting temperature of cuprous chloride (CuCl) at 430°C, 2) the non-transparent dark grey colour of molten CuCl, which obstructs the visibility of oxygen bubbles, 3) the highly corrosive nature of molten cuprous chloride, 4) the strong oxidizing property of oxygen gas, which can lead to rapid combustion of materials, and 5) the high-temperature process involved. To overcome these challenges, alternative materials have been identified using dimensional analysis to simulate the hydrodynamic and heat transfer behaviours of the actual materials. Liquid water at 22±2°C and helium gas at 90±2°C have been found to be suitable substitutes. These alternative materials not only provide a safer environment for experiments but also allow for lower operating temperatures. Moreover, they are readily available and more cost-effective (Abdulrahman, 2019a, 2020a).

The experimental studies of the oxygen reactor have shed light on key aspects of SBCRs, including transition velocity, overall gas holdup, and direct contact heat transfer, providing valuable insights for optimizing their performance (Abdulrahman, 2015, 2016a, 2016d, 2016e, 2018). In the study of the transition velocity, which marks the shift from homogeneous to churn turbulent flow regimes within the reactor, the experiments revealed that the transition velocity decreases with an increase in static liquid height and solid concentration. This finding suggests that the physical dimensions of the reactor and the density of the slurry play significant roles in determining the flow regime. Also, the research indicated that slug flow, a regime characterized by large gas bubbles, is not typically present in industrial SBCRs (Abdulrahman, 2016e).

Another important aspect investigated experimentally is the overall gas holdup, which refers to the volume fraction of gas within the reactor. This parameter is crucial for

assessing the reactor's efficiency and capacity for mass transfer. The experimental study found that the overall gas holdup increases with the superficial gas velocity, particularly at lower velocities. However, it decreases with increasing static liquid height and solid concentration. Interestingly, the impact of solid particle diameter on gas holdup was found to be negligible, suggesting that particle size might not be a critical factor in certain operating conditions (Abdulrahman, 2016d).

Direct contact heat transfer in SBCRs, is a process vital for maintaining optimal reaction temperatures and energy efficiency. The experimental results showed that both the volumetric heat transfer coefficient and the slurry temperature increase with the superficial gas velocity, with a more pronounced effect at lower velocities. Conversely, these parameters decrease with an increase in static liquid height and solid concentration. The findings imply that manipulating the gas flow rate and reactor dimensions can effectively control heat transfer within the system (Abdulrahman, 2015). The schematic diagram of the SBC experimental setup is illustrated in Fig.1 and the dimensions of the reactor column and sparger used in the experiments are shown in Figs. 2 and 3 respectively.

The experimental studies provide a deeper understanding of the complex dynamics within slurry bubble column reactors. By elucidating the relationships between key operating parameters and reactor performance, these findings offer valuable guidance for designing and optimizing SBCRs in various industrial applications. For instance, adjusting the static liquid height and solid concentration can help regulate the transition velocity and gas holdup, while controlling the superficial gas velocity can optimize heat transfer efficiency.

Fig. 1 Schematic diagram of the experimental setup (Abdulrahman, 2016a).
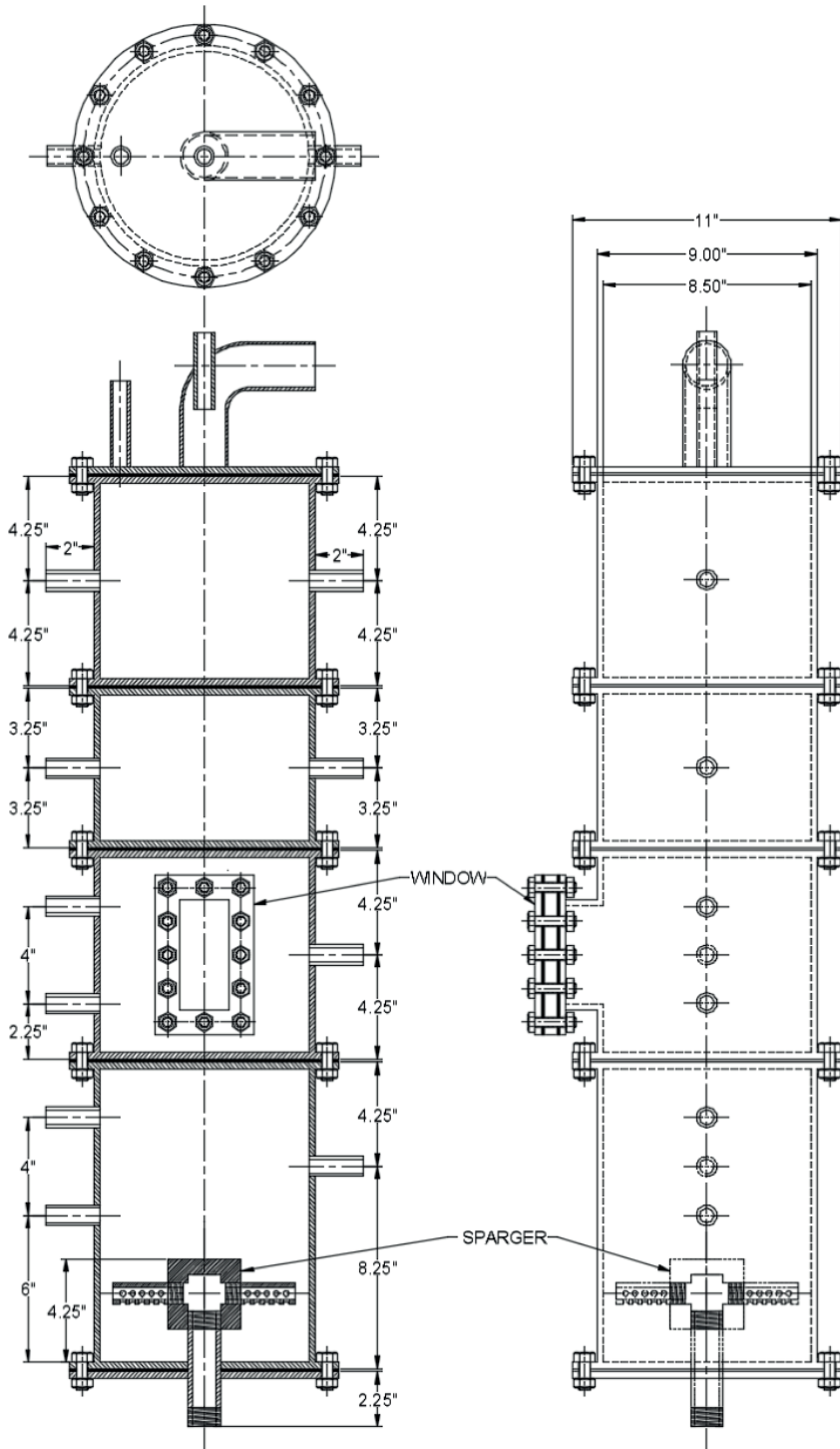
Fig. 2 Reactor column dimensions (Abdulrahman, 2016a).

Bottom Sectional View

Top Sectional View

Top View

Side Sectional View
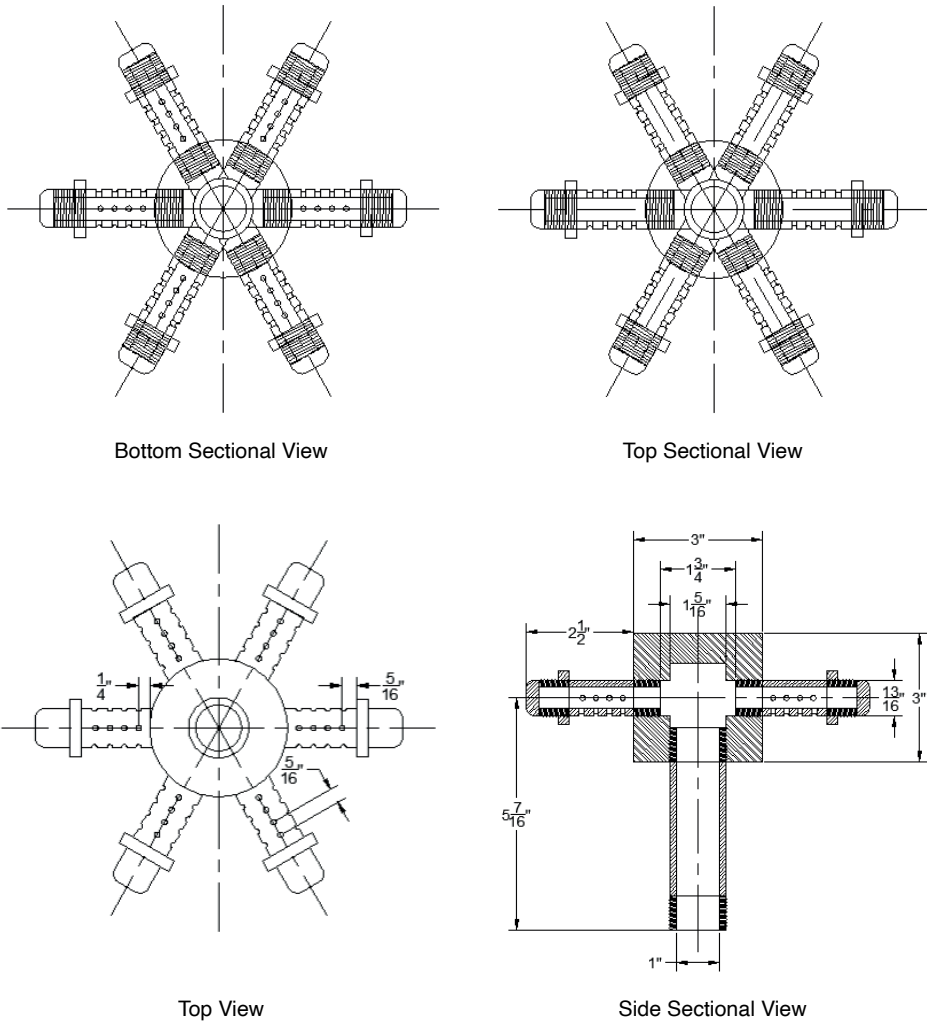
Fig. 3 Dimensions of the sparger (Abdulrahman, 2016a).

CFD Studies

The objective of the Computational Fluid Dynamics (CFD) simulations of direct contact heat transfer in the multiphase oxygen reactor, is to enhance our understanding of the hydrodynamics and heat transfer phenomena within these reactors. A comprehensive review of Eulerian CFD approaches for analysing BCR/SBCRs has highlighted the accuracy of these models in predicting reactor performance. Key findings include the increase in gas holdup with superficial gas velocity, column pressure, and gas phase density, and the uneven distribution of gas holdup within the reactor (Abdulrahman, 2022d).

One area of focus in CFD studies, is the volumetric heat transfer coefficient in SBCRs, where helium gas is injected through a slurry of water and alumina solid particles.

Researchers have investigated the effects of superficial gas velocity, static liquid height, and solid particle concentration on the volumetric heat transfer coefficient. CFD simulations revealed that the heat transfer coefficient increases with superficial gas velocity and decreases with higher static liquid height or solid concentration. These findings are crucial for optimizing reactor design and operation for efficient heat transfer (Abdulrahman, 2016f).

Temperature distribution within the slurry is another aspect that has been explored through 2D CFD simulations. Similar to the heat transfer coefficient, the average slurry temperature rises with increased superficial gas velocity and drops with higher static liquid height or solid concentration. However, the impact of solid concentration on temperature is found to be negligible. These insights are valuable for maintaining optimal reactor temperatures for various chemical processes (Abdulrahman, 2016g, 2020b, 2020c, 2022b).

Finally, the overall gas holdup in helium-water bubble columns has also been predicted using 2D and 3D CFD simulations. Results indicate that gas holdup increases with superficial gas velocity and decreases with higher static liquid height. The three-dimensional model was found to be more accurate for gas holdup in comparison to the two-dimensional model. This information is essential for scaling up bubble column reactors, as gas holdup is a key parameter describing reactor performance (Nassar, 2023; Abdulrahman & Nassar, 2023a, 2023b, 2023c).

In Table 2, the equations utilized in the CFD analysis are displayed. Table 2 contains equations that are explicitly expressed in gas phase. Since the equations for the liquid phase are comparable to those for the gas phase, they are not repeated. Table 3 summarizes the setup used in the simulations.

Description	Equation
Volume equation (Abdulrahman, 2019c)	$V_g = \int_V \alpha_g \, dV$
Continuity equation in 3D Polar coordinates (r, θ, y) (Harvego, 2006)	$\nabla \cdot V_g = \frac{\partial v_{r,g}}{\partial r} + \frac{v_{r,g}}{r} + \frac{1}{r}\frac{\partial v_{\theta,g}}{\partial \theta} + \frac{\partial v_{y,g}}{\partial y} = 0$
Momentum equation in 3D Polar coordinates (Harvego, 2006)	$\rho_g \alpha_g \left(\frac{\partial v_r}{\partial t} + v_r \frac{\partial v_r}{\partial r} + \frac{v_\theta}{r}\frac{\partial v_r}{\partial \theta} + vy \frac{\partial v_r}{\partial y} - \frac{v_\theta^2}{r}\right) = -\alpha_g \frac{\partial P}{\partial r} +$ $\alpha_g \frac{\mu_{g,eff}}{3}\frac{\partial (\nabla \cdot V)}{\partial r} + \mu_{g,eff}\, \alpha_g \left[\frac{1}{r}\frac{\partial}{\partial r}\left(r \frac{\partial v_r}{\partial r}\right) + \frac{1}{r^2}\frac{\partial^2 v_r}{\partial \theta^2} + \frac{\partial^2 v_r}{\partial y^2} - \frac{v_r}{r^2} -$ $\frac{2}{r^2}\frac{\partial v_\theta}{\partial \theta}\right] + \rho_g \alpha_g \, g_r + M_{i,g,r}$ $\rho_g \alpha_g \left(\frac{\partial v_\theta}{\partial t} + v_r \frac{\partial v_\theta}{\partial r} + \frac{v_\theta}{r}\frac{\partial v_\theta}{\partial \theta} + v_y \frac{\partial v_\theta}{\partial y} + \frac{v_r v_\theta}{r}\right) = -\alpha_g \frac{1}{r}\frac{\partial P}{\partial \theta} +$ $\alpha_g \frac{\mu_{g,eff}}{3r}\frac{\partial (\nabla \cdot V)}{\partial \theta} + \alpha_g \mu_{g,eff}\left[\frac{1}{r}\frac{\partial}{\partial r}\left(r \frac{\partial v_\theta}{\partial r}\right) + \frac{1}{r^2}\frac{\partial^2 v_\theta}{\partial \theta^2} + \frac{\partial^2 v_\theta}{\partial y^2} +$ $\frac{2}{r^2}\frac{\partial v_r}{\partial \theta} - \frac{v_\theta}{r^2}\right] + \rho_g \alpha_g \, g_\theta + M_{i,g,\theta}$ $\rho_g \alpha_g \left(\frac{\partial v_y}{\partial t} + v_r \frac{\partial v_y}{\partial r} + \frac{v_\theta}{r}\frac{\partial v_y}{\partial \theta} + v_y \frac{\partial v_y}{\partial y}\right) = -\alpha_g \frac{\partial P}{\partial y} +$ $\alpha_g \, \mu_{g,eff}\left[\frac{1}{r}\frac{\partial}{\partial r}\left(r \frac{\partial v_y}{\partial r}\right) + \frac{1}{r^2}\frac{\partial^2 v_y}{\partial \theta^2} + \frac{\partial^2 v_y}{\partial y^2}\right] + \rho_g \alpha_g g_y + M_{i,g,y}$
Energy equation in 3D Polar coordinates (Harvego, 2006)	$\alpha_g \rho_g C \left(\frac{\partial T_g}{\partial t} + v_{r,g}\frac{\partial T_g}{\partial r} + \frac{v_{\theta,g}}{r}\frac{\partial T_g}{\partial \theta} + v_{y,g}\frac{\partial T_g}{\partial y}\right) = \bar{\bar{\tau}}_g : \nabla V_g +$ $k_g \left(\frac{1}{r}\frac{\partial}{\partial r}\left(r \frac{\partial T_g}{\partial r}\right) + \frac{1}{r^2}\frac{\partial^2 T_g}{\partial \theta^2} + \frac{\partial^2 T_g}{\partial y^2}\right) + S_g + Q_{g,sl}$
Effective density	$\hat{\rho}_g = \alpha_g \, \rho_g$
Drag force (Abdulrahman, 2019c)	$M_D = \frac{\rho_g f}{6 \, \tau_b} \, d_b \, A_i \left(V_g - V_l\right)$
Interfacial area (Abdulrahman, 2019c)	$A_i = \frac{6 \, \alpha_g \, (1 - \alpha_g)}{d_b}$
Schiller-Naumann drag equation (Abdulrahman, 2013b)	$C_D = \begin{cases} \frac{24 \, (1 + 0.15 \, Re_b^{0.687})}{Re_b} & Re_b \leq 1000 \\ 0.44 & Re_b > 1000 \end{cases}$

Table 2: Details of equations used in the 3D CFD simulations (Abdulrahman & Nassar, 2023a).

General	Solver Type	Pressure-Based	
	Velocity Formulation	Absolute	
	Time	Steady	
	Gravity	ON	
Models	Multiphase-Eulerian		
	Energy-On		
	Viscous-Standard k - ε, Standard Wall Function, Dispersed		
Materials	Water liquid		
	Helium gas		
Phases	Primary phase=liquid phase		
	Secondary Phase=gas phase		
Bubble Diameter	Sauter-mean diameter		
Solution Methods	Scheme	Phase-Coupled SIMPLE	
	Spatial Discretization	Gradient	Least Squares Cell Based
		Momentum	Second Order Upwind
		Volume Fraction	First Order Upwind
		Turbulent Kinetic Energy	Second Order Upwind
		Turbulent Dissipation Rate	Second Order Upwind
		Energy	Second Order Upwind
		Interfacial Area Concentration	Second Order Upwind

Table 2 Summary of the SBCR problem setup (Abdulrahman, 2016f).

In conclusion, CFD simulations have provided valuable insights into the hydrodynamics and heat transfer in slurry bubble column reactors. These advancements are instrumental in optimizing reactor designs and operations for various industrial applications, particularly in hydrogen production, contributing to the development of sustainable energy technologies. The results of both the experimental and CFD works are shown in Table 4.

Volumetric Heat Transfer Coefficient	Average Slurry Temperature	Overall Gas Holdup	Transition Velocity
Increases by increasing the superficial gas velocity with a higher rate of increase at lower superficial gas velocity.			In the industrial SBCRs, the slug flow regime does not exist and there is only one transition velocity, which is between the homogeneous and heterogeneous flow regimes.
Decreases by increasing the static liquid height.			
Decreases by increasing solid concentration.	The decrease of the slurry temperature with the solid concentration is negligible.	Decreases by increasing solid concentration and at a higher solid concentration, the changing rate of the overall gas holdup with the superficial gas velocity and/or the solid concentration is lower. The effect of the solid particle diameter on overall gas holdup is negligible.	Decreases by increasing solid concentration.
The rate of decrease with the solid concentration are approximately the same for different superficial gas velocities.		The distribution along the cross-section of the column is unequal, where the gas holdup is higher at the centre of the column and lower near the wall region.	
Profiles calculated from CFD models, generally under-predicted the experimental data of Abdulrahman (2015, 2016d, 2016f).			
The CFD models correctly predicted the effects of superficial gas velocity, static liquid height and solid concentration.			
The CFD results were validated for superficial gas velocities up to 0.15 m/s, and aspect ratios up to 4.			

Table 4: Results of experimental and CFD analyses for direct contact heat transfer (Abdulrahman, 2022c).

CONCLUSIONS

Recent improvements in the multiphase oxygen reactor for the copper-chlorine thermochemical cycle were presented and assessed in this review work. The study identified previous experimental and theoretical findings acquired from research groups working on the development of scaled-up oxygen reactor facilities. The oxygen reactor's type and description were discussed in details and it is concluded that using SBCR is the best option for the oxygen reactor. Oxygen production chemical reaction was described in details and it was found that the reaction is an endothermic reaction with a reaction heat of 129.2 kJ/mol and a temperature of 530°C which is the highest temperature in the Cu-Cl

cycle. The source of heat can be from nuclear reactors or solar energy sources. Also, the material properties of the oxygen reactor contents were extensively explained. Moreover, the factors that affect the size of the oxygen reactor were discussed. The factors include the residence time of the thermal decomposition for solid particles, terminal settling velocity of solid particles, production rate of hydrogen, and reactor heating rate. The techniques of heat transfer required by the oxygen reactor, such as indirect and direct contact heat transfer, were also analysed in this study. It was concluded that using direct contact heat transfer is preferred to indirect heat transfer methods.

REFERENCES

Abdulrahman, M. W. (2015). **Experimental studies of direct contact heat transfer in a slurry bubble column at high gas temperature of a helium–water–alumina system**. *Applied Thermal Engineering*, *91*, 515-524.

Abdulrahman, M. W. (2016a). ***Analysis of the thermal hydraulics of a multiphase oxygen production reactor in the Cu-Cl cycle***. University of Ontario Institute of Technology (Canada).

Abdulrahman, M. W. (2016b). **Similitude for thermal scale-up of a multiphase thermolysis reactor in the cu-cl cycle of a hydrogen production**. *World Academy of Science, Engineering and Technology, International Journal of Electrical, Computer, Energetic, Electronic and Communication Engineering*, *10*(5), 567-573.

Abdulrahman, M. W. (2016c). **Heat transfer analysis of a multiphase oxygen reactor heated by a helical tube in the cu-cl cycle of a hydrogen production**. *World Academy of Science, Engineering and Technology, International Journal of Mechanical, Aerospace, Industrial, Mechatronic and Manufacturing Engineering*, *10*(6), 1018-1023.

Abdulrahman, M. W. (2016d). **Experimental studies of gas holdup in a slurry bubble column at high gas temperature of a helium– water– alumina system**. *Chemical Engineering Research and Design*, *109*, 486-494.

Abdulrahman, M. W. (2016e). **Experimental studies of the transition velocity in a slurry bubble column at high gas temperature of a helium–water–alumina system**. *Experimental Thermal and Fluid Science*, *74*, 404-410.

Abdulrahman, M. W. (2016f). **CFD simulations of direct contact volumetric heat transfer coefficient in a slurry bubble column at a high gas temperature of a helium–water–alumina system**. *Applied thermal engineering*, *99*, 224-234.

Abdulrahman, M. W. (2016g). **CFD Analysis of Temperature Distributions in a Slurry Bubble Column with Direct Contact Heat Transfer**. In *Proceedings of the 3rd International Conference on Fluid Flow, Heat and Mass Transfer (FFHMT'16)*.

Abdulrahman, M. W. (2018). *U.S. Patent No. 10,059,586*. Washington, DC: U.S. Patent and Trademark Office.

Abdulrahman, M. W. (2019a). **Simulation of Materials Used in the Multiphase Oxygen Reactor of Hydrogen Production Cu-Cl Cycle**. In *Proceedings of the 6 the International Conference of Fluid Flow, Heat and Mass Transfer (FFHMT'19)* (pp. 123-1).

Abdulrahman, M. W. (2019b). **Heat transfer in a tubular reforming catalyst bed: Analytical modelling**. In *proceedings of the 6th International Conference of Fluid Flow, Heat and Mass Transfer*.

Abdulrahman, M. W. (2019c). **Exact analytical solution for two-dimensional heat transfer equation through a packed bed reactor**. In *Proceedings of the 7th World Congress on Mechanical, Chemical, and Material Engineering*.

Abdulrahman, M. W. (2020a). *U.S. Patent No. 10,526,201*. Washington, DC: U.S. Patent and Trademark Office.

Abdulrahman, M. W. (2020b). **Effect of Solid Particles on Gas Holdup in a Slurry Bubble Column**. In *Proceedings of the 6th World Congress on Mechanical, Chemical, and Material Engineering*.

Abdulrahman, M. W. (2020c). **CFD Simulations of Gas Holdup in a Bubble Column at High Gas Temperature of a Helium-Water System**. In *Proceedings of the 7th World Congress on Mechanical, Chemical, and Material Engineering (MCM'20)* (pp. 169-1).

Abdulrahman, M. W. (2022a). **Heat Transfer Analysis of the Spiral Baffled Jacketed Multiphase Oxygen Reactor in the Hydrogen Production Cu-Cl Cycle**. In *Proceedings of the 9th International Conference on Fluid Flow, Heat and Mass Transfer (FFHMT'22)*.

Abdulrahman, M. W. (2022b). **Temperature profiles of a direct contact heat transfer in a slurry bubble column**. *Chemical Engineering Research and Design*, *182*, 183-193.

Abdulrahman, M. W. (2022c). **Review of the Thermal Hydraulics of Multi-Phase Oxygen Production Reactor in the Cu-Cl Cycle of Hydrogen Production**. In *Proceedings of the 9th International Conference on Fluid Flow, Heat and Mass Transfer (FFHMT'22)*.

Abdulrahman, M. W., & Nassar, N. (2022d). **Eulerian Approach to CFD Analysis of a Bubble Column Reactor–A Review**. In *Proceedings of the 8th World Congress on Mechanical, Chemical, and Material Engineering (MCM'22)*.

Abdulrahman, M. W., & Nassar, N. I. (2023a). **A Three-Dimensional CFD Analyses for the Gas Holdup in a Bubble Column Reactor**. In *Proceedings of the 9th World Congress on Mechanical, Chemical, and Material Engineering (MCM'23)*.

Abdulrahman, M. W., & Nassar, N. I. (2023b). **Three Dimensional CFD Analyses for the Effect of Solid Concentration on Gas Holdup in a Slurry Bubble Column**. In *Proceedings of the 9th World Congress on Mechanical, Chemical, and Material Engineering (MCM'23)*.

Abdulrahman, M. W., & Nassar, N. I. (2023c). **Effect of Static Liquid Height on Gas Holdup of a Bubble Column Reactor**. In *Proceedings of the 9th World Congress on Mechanical, Chemical, and Material Engineering (MCM'23)*.

Abdulrahman, M. W., Wang, Z., & Naterer, G. F. (2013a). **Scale-up analysis of three-phase oxygen reactor in the Cu-Cl thermochemical cycle of hydrogen production**. In *EIC Climate Change Technology Conference*.

Abdulrahman, M. W., Wang, Z., Naterer, G. F., & Agelin-Chaab, M. (2013b). **Thermohydraulics of a thermolysis reactor and heat exchangers in the Cu-Cl cycle of nuclear hydrogen production**. In *Proceedings of the 5th World Hydrogen Technologies Convention*.

Baldi, G., Conti, R., & Alaria, E. (1978). **Complete suspension of particles in mechanically agitated vessels**. *Chemical Engineering Science*, *33*(1), 21-25.

De Micco, G., Bohé, A. E., & Pasquevich, D. M. (2007). **A thermogravimetric study of copper chlorination**. *Journal of alloys and compounds*, *437*(1-2), 351-359.

Di Felice, R., & Kehlenbeck, R. (2000). **Sedimentation velocity of solids in finite size vessels**. *Chemical Engineering & Technology: Industrial Chemistry-Plant Equipment-Process Engineering-Biotechnology*, *23*(12), 1123-1126.

Forsberg, C. W. (2007). **Future hydrogen markets for large-scale hydrogen production systems**. *International Journal of Hydrogen Energy*, *32*(4), 431-439.

Harvego, E. A. (2006). ***Evaluation of next generation nuclear power plant (NGNP) intermediate heat exchanger (IHX) operating conditions* (No. INL/EXT-06-11109)**. Idaho National Lab.(INL), Idaho Falls, ID (United States).

Ikeda, B. M., & Kaye, M. H. (2008, August). **Thermodynamic properties in the Cu-Cl-OH system**. In *7th International conference on nuclear and radiochemistry, Budapest, Hungary*.

Janz, G. J., & Tomkins, R. P. T. (1983). Molten salts: volume 5, Part 2. **Additional single and multi-component salt systems. Electrical conductance, density, viscosity and surface tension data**. *Journal of physical and chemical reference data*, *12*(3), 591-815.

Lewis, M. A., Masin, J. G., & Vilim, R. B. (2005). **Development of the low temperature Cu-Cl thermochemical cycle**. *Argonne National Laboratory, International Congress on Advances in Nuclear Power Plants*, Seoul, Korea.

Lewis, M. A., Serban, M., & Basco, J. K. (2003). **Generating hydrogen using a low temperature thermochemical cycle**. In *Proceedings of the ANS/ENS 2003 Global International Conference on Nuclear Technology, New Orleans*.

Li, X., Zhang, L., Nakaya, M., & Takenaka, A. (2016, October). **Application of economic MPC to a CSTR process**. In *2016 IEEE Advanced Information Management, Communicates, Electronic and Automation Control Conference (IMCEC)* (pp. 685-690). IEEE.

Marin, G. D. (2012). ***Kinetics and transport phenomena in the chemical decomposition of copper oxychloride in the thermochemical Cu-Cl Cycle*** (Doctoral dissertation).

Nassar, N. I. (2023). ***A Three-Dimensional CFD Analyses for the Hydrodynamics of the Direct Contact Heat Transfer in the Oxygen Production Slurry Bubble Column Reactor of the Cu-Cl Cycle of Hydrogen Production***. Rochester Institute of Technology.

Natesan, K., Moisseytsev, A., & Majumdar, S. (2009). **Preliminary issues associated with the next generation nuclear plant intermediate heat exchanger design**. *Journal of nuclear materials*, *392*(2), 307-315.

Nguyen, A., & Schulze, H. J. (2003). ***Colloidal science of flotation***. CRC press.

Oldshue, J. Y. (1983). **Fluid mixing technology**.

Parry, T. J. (2008). *I. Thermodynamics and Magnetism of Cu 2 OCl 2 II. Repairs to Microcalorimeter*. Brigham Young University.

Richardson, J. F. (1954). u. WN Zaki: **Sedimentation and fluidization**. *Trans. Instn. chem. Engrs. Bd*, *32*, 35.

Ryskamp, J. M., Hildebrandt, P., Baba, O., Ballinger, R., Brodsky, R., Chi, H. W., ... & Lensa, W. V. (2004). ***Design Features and Technology Uncertainties for the Next Generation Nuclear Plant*** **(No. INEEL/EXT-04-01816)**. Idaho National Lab.(INL), Idaho Falls, ID (United States).

Serban, M., Lewis, M. A., & Basco, J. K. (2004). ***Kinetic study of the hydrogen and oxygen production reactions in the copper-chloride thermochemical cycle***. American Institute of Chemical Engineers.

Trevani, L. (2011, May). **The copper-chloride cycle: synthesis and characterization of copper oxychloride**. In *Hydrogen and Fuel Cells International Conference and Exhibition*.